The Interpretation of Short Climate Records, with Comments on the North Atlantic and Southern Oscillations

Carl Wunsch
Program in Atmospheres, Oceans, and Climate, Department of Earth, Atmospheric, and Planetary Sciences, Massachusetts Institute of Technology, Cambridge, Massachusetts

ABSTRACT

This pedagogical note reminds the reader that the interpretation of climate records is dependent upon understanding the behavior of stochastic processes. In particular, before concluding that one is seeing evidence for trends, shifts in the mean, or changes in oscillation periods, one must rule out the purely random fluctuations expected from stationary time series. The example of the North Atlantic oscillation (NAO) is mainly used here: the spectral density is nearly white (frequency power law $\approx s^{-0.2}$) with slight broadband features near 8 and 2.5 yr. By generating synthetic but stationary time series, one can see exhibited many of the features sometimes exciting attention as being of causal climate significance. Such a display does not disprove the hypothesis of climate change, but it provides a simple null hypothesis for what is seen. In addition, it is shown that the linear predictive skill for the NAO index must be very slight (less than 3% of the variance). A brief comparison with the Southern Oscillation shows a different spectral distribution, but again a simulation has long periods of apparent systematic sign and trends. Application of threshold-crossing statistics (Ricean) shows no contradiction to the assumption that the Darwin pressure record is statistically stationary.

1. Introduction

The intense interest in possible climate change has led to increasing scrutiny of relatively long time series for indications of secular trends in climate indicators. Changes in mean levels of simple fields such as temperature, or shifts in the apparent return times (or oscillation periods) of various phenomena such as the El Niño–Southern Oscillation (ENSO) or the North Atlantic oscillation (NAO), have all been discussed.

But purely random processes, particularly those that have even mildly "red" spectra, have a behavior that comes as a surprise to many, and there is great risk of misinterpretation. That is, the purely random behavior of a rigorously stationary process often appears visually interesting, particularly over brief time intervals, and creates the temptation to interpret it as arising from specific and exciting deterministic causes. The issue is related to the often unintuitive behavior of systems undergoing random walk (e.g., Feller 1957; Hasselmann 1977; Frankignoul and Hasselmann 1977; Wunsch 1992).

There is nothing here that will be regarded as new by practitioners of time series analysis in a wide geophysical context (this paper started out as a classroom note). My intention is to simply introduce a bit of caution into an important discussion of the behavior of climate signals.

In what follows, I explore some of the behavior of the simplest of all time series, those that have a normal probability density and are stationary (i.e., having statistics that do not change in time). Here "wide-sense stationarity," requiring only that the first and second moments be time independent, is adequate. Climate surely exhibits nonstationary, nonlinear/nonnormal behavior, but one should be very careful

Corresponding author address: Carl Wunsch, Program in Atmospheres, Oceans, and Climate, Department of Earth, Atmospheric, and Planetary Sciences, Massachusetts Institute of Technology, Cambridge, MA 02139.
E-mail: cwunsch@pond.mit.edu
In final form 1 October 1998.

before rejecting, on the basis of visual intuition, the null hypothesis of stationarity. In particular, distinguishing nonstationarity (which many have sought to display in the present climate system) from nonnormality is extremely difficult.

2. An example: Weakly red noise

Let z_t be the so-called NAO index, here taken to be the atmospheric pressure difference between Lisbon and Iceland averaged over the winter months (December–March) and displayed in Fig. 1. The interval covered is 133 yr: 1864–1996 (see Hurrell 1995; Goodman 1997). Also displayed is a filtered version of z_t with energy at periods shorter than 4 yr having been removed. There are intervals, most clearly visible in the filtered time series, of extended residence both above and below the mean, and a period, particularly since about 1960, of an apparent trend.

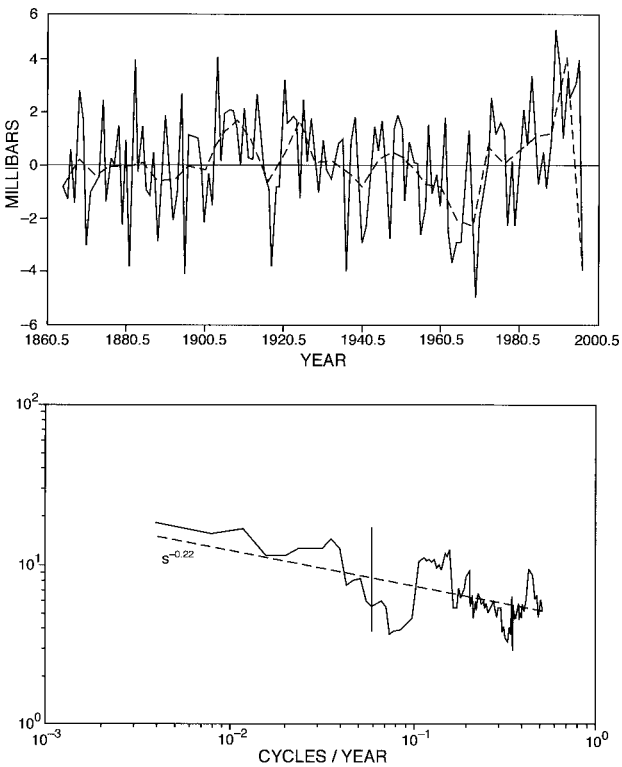

FIG. 1. (top) Solid line is the winter-average Lisbon minus Iceland pressure difference from 1864 to 1996, z_t (Hurrell 1995; Goodman 1997), here called the "NAO index." Dashed line is the running 4-yr averaged values (as obtained from an eighth-order Chebyshev filter). The latter spends extended periods above (e.g., about 1968–95) or below (e.g., 1950–67) the mean. The shift between these two states might be interpreted as a trend; whether it is truly secular in nature remains to be seen. (bottom) Multitaper spectral density estimate (Percival and Walden 1993) $\Phi(s)$ as a function of angular frequency s of the data in Fig. 1a. This and other 95% confidence intervals are the mean interval for all the spectral estimates, the procedure being an adaptive one. The dashed line showing an average power law behavior was obtained from a simple least squares fit. Because of the logarithmic frequency scale, most of the record energy lies at the high-frequency end of the scale.

The estimated power density spectrum $\Phi(s)$ as a function of angular frequency s for z_t computed using D. Thomson's multitaper method (see Percival and Walden 1993) is shown in Fig. 1. The spectrum is very weakly red, increasing slowly with increasing period, with a slight, but apparently statistically significant, structure. The variance of z_t is $\sigma^2 = 3.8$ mb^2. A least squares fit produces a power law,

$$\Phi^{(r)}(s) \approx 0.66 s^{-0.22} \text{ mb}^2/\text{cycle/yr}, \qquad (1)$$

in the range shown on the figure. There are weak structures in the range of 8–10 yr and near 2 yr. Note that most of the energy in such a record occurs at the highest frequencies, a behavior obscured by the logarithmic frequency scale used to plot the power density spectral estimate.

The exploration strategy here is to produce artificial, statistically unchanging time series whose power density spectra are consistent with what is observed for the NAO and to examine the way such time series behave over time.[1] Let us examine the behavior of a sequence of values, y_t, whose spectral density is given by (1). Four 133-yr intervals chosen arbitrarily from within a longer time span from the resulting time series can be seen in Fig. 2. It was confirmed that the result did have a power density spectrum, within expected confidence limits, of $\Phi^{(r)}(s)$. Similar, but different, simulations have been published by others for the Southern Oscillation (SO); these are discussed briefly at the end.

[1]A zero-mean time series of duration 4096 "years" was generated by synthesis of the Fourier series,

$$y_t = \sum_{n=1}^{[T/2]} a_n \cos\left(\frac{2\pi nt}{T}\right) + \sum_{n=1}^{[T/2]-1} b_n \sin\left(\frac{2\pi nt}{T}\right), \quad T = 4097,$$

where a_n, b_n were generated by a Gaussian pseudorandom number generator such that $< a_n > = < b_n > = 0$, $< a^2_n > = < b^2_n > = \Phi^{(r)}(s = n/T)/2$, $< a_n a_m > = < b_n b_m > = 0$, $m \neq n$, $< a_n b_m > = 0$. The requirements on the a_n, b_n assure wide-sense stationarity. Confirmation of stationarity, and that the appropriate spectral density is reproduced, can be simply obtained by considering the behavior of the autocovariance $< y_t y_q >$ (see Percival and Walden 1993). A unit time step, $t = 0, 1, 2, \ldots$, is used.

Because of the visual noisiness of the result, Fig. 2 shows four subintervals of 133 yr of the time series filtered so as to remove all energy at periods shorter than 4 yr. Notice that there are again extended periods when the filtered time series is resident far from the zero mean. Such a result, in isolation, could easily be interpreted as representing a new climate state. To the extent that the NAO index produces like behavior, the weather and climate of western Europe would be substantially different. The simulation shows, however, that there need not be any specific cause for this shift; it is merely the expected behavior of a weakly red noise process and has no "cause" any more than does a sequence of rolls of dice that produces a statistical excess of the value six.

Results such as those shown in Fig. 2 can be studied analytically, a subject that has a large literature, often traced back to the classic paper of Rice (1945). For example, Vanmarcke (1983, chap. 4) has a discussion of expected time series excursions for Gaussian processes. Claims that one has entered a new climate state because of extended excursions away from the mean need to be tested against the null hypothesis that the extreme duration is expected to occur by chance at some particular confidence level. Some of the ideas emerging from Ricean statistics will be explored briefly at the end.

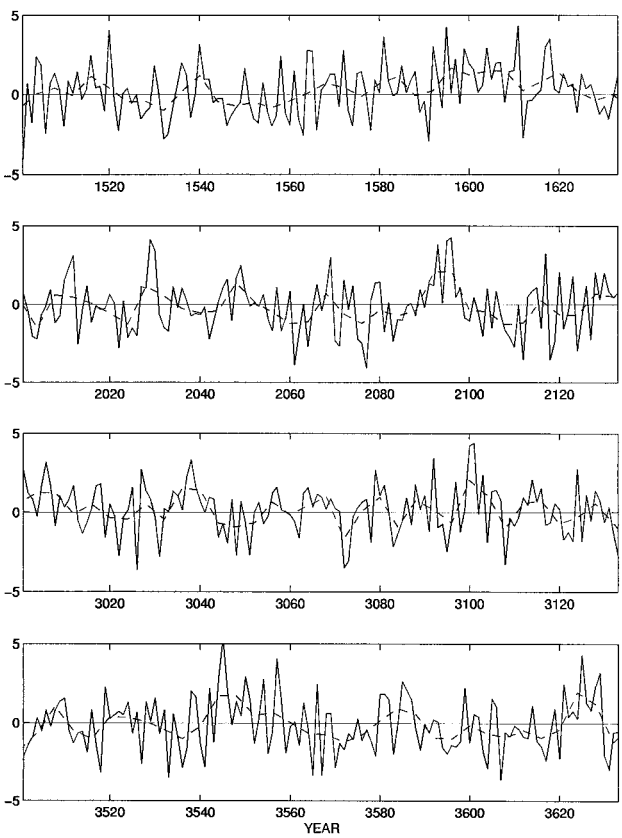

FIG. 2. Simulated data, having a red noise spectrum proportional to $s^{-0.22}$ with the same variance as z_t, plotted in four sections of 133 yr each (solid line). The dashed line shows the 4-yr average time series obtained with filtering identical to that applied to z_t. As in Fig. 1b, there are extended periods in which the filtered values remain far from the mean (e.g., about 1570–1620, in the first panel, or 2055–90 in the second panel).

3. Example with the structured spectrum

Figure 1b indicates that there are weak structures (calling them "peaks" seems too strong) in the spectrum of the actual NAO index. Although the amount of energy lying in the frequency bands of the structures is not very large, less than about 10%, it seems worthwhile to generate time series with the full spectrum $\Phi(s)$. Another time series, y_t, was produced as above except for use of the numerically specified

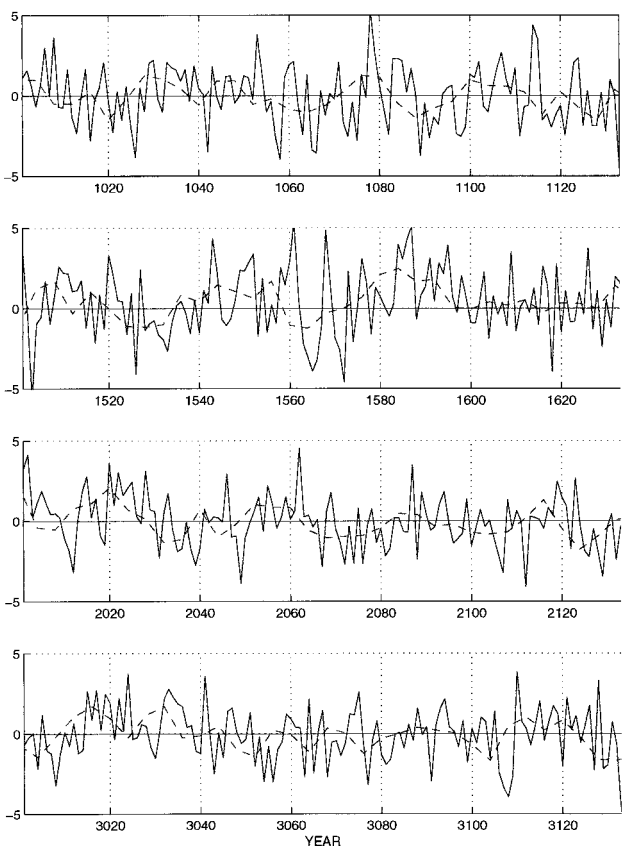

FIG. 3. Simulated data, with a spectral density equal to the full curve in Fig. 1b, both unfiltered (solid) and filtered. There are again periods of a single sign in the filtered data and even of local trends (e.g., about 1570–85).

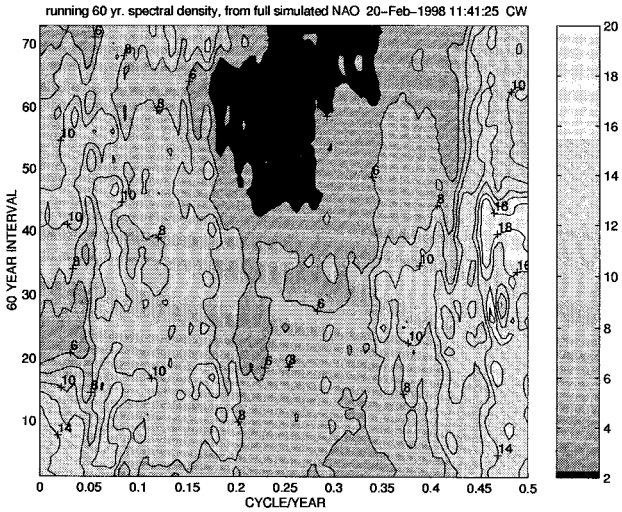

FIG. 4. Power density spectrum for successive 60-yr periods, each shifted by 1 yr relative to the previous, from an arbitrary 133-yr segment of the realization of z_t. Here the frequency scale is linear as are contour intervals in units of mb^2/cycle /yr^{-1}. [The time axis has the opposite sense of that of Hurrell and van Loon (1997), but because z_t is stationary the change makes no difference.]

spectral density in Fig. 1. Figure 3 again shows arbitrary 133-yr records with a similar behavior of extended excursions from the mean and local apparent trends.

Using Fig. 3, we can locate regions in which the character of the high-frequency oscillations appears to change, for example, in the two 20-yr periods beginning around the year 3000 in which an interval of high-frequency dominance gives way to one of apparent low-frequency dominance. (One can count peaks in the various 20-yr blocks to obtain such indicators.)

Hurrell and van Loon (1997) displayed a so-called spectrogram for z_t (the spectral density computed in a sliding 60-yr window starting in 1865–1924 and ending with 1935–94) and suggested that the NAO spectrum had become redder in recent years. Here, an arbitrary 133-yr period was used to compute a similar set of estimates for y_t. The result is shown in Fig. 4. Consider the frequency range from about 0.2 to 0.3 cycles yr^{-1}. In that band, the energy level changes by about a factor of 4 from the 60-yr intervals at the beginning of the 133-yr period to the ones near the end. Factor of 2 changes are also seen, for example, near periods of 2 yr (0.5 cycle /year^{-1}) where these oscillations appear unusually energetic around the 40th interval. A similar behavior is seen near 0.04 cycles yr^{-1} (25-yr period). Again, the time series was statistically stationary, and these fluctuations have no physical cause other than random superposition; neither is there any significance to the particular frequency ranges where they have appeared.

One must also be wary of apparent trends. For example, the interval in Fig. 3 from about 3020 to 3050 could look to an observer with a short record as indicating a general decline in the NAO index. The much longer synthetic record shows, however, that it is nothing but the swing expected of a stochastic process.

4. Prediction

If the NAO process is essentialy linear, then the extent of its predictability can be understood in an elementary way from its spectral density and the theory of discrete Wiener filtering (see Levinson 1947; Claerbout 1976). Write

$$z_t = \sum_{k=0}^{K} a_k \theta_{t-k},\ a_0 = 1, \tag{2}$$

where θ_t is a stationary, zero mean white noise process of variance $< \theta_t^2 = \sigma_\theta^2$ and a_k is a special, specific, deterministic sequence. This "predictive decomposition" for the NAO can always be constructed, and it permits one to make a best prediction one time step (here 1 yr) in the future. Equation (2) is a special case of a so-called moving average (MA) process, and it can be easily converted, see, for example, Box et al. (1994), into a corresponding autoregressive, or autoregressive/moving average (ARMA) process. Because

$$z_{t+1} = \theta_{t+1} + \sum_{k=1}^{K} a_k \theta_{t+1-k} \tag{3}$$

by Eq. (2), and θ_{t+1} is unknown and unpredictable, the best prediction is

$$\tilde{z}_{t+1} = 0 + \sum_{k=1}^{K} a_k \theta_{t+1-k}, \tag{4}$$

with expected error (see appendix)

$$< (\tilde{z}_{t+1} - z_t)^2 > = < \theta_{t+1}^2 > = \sigma_\theta^2. \tag{5}$$

If z_t is itself white noise, only a_0 is nonvanishing. A structured covariance produces larger K and hence

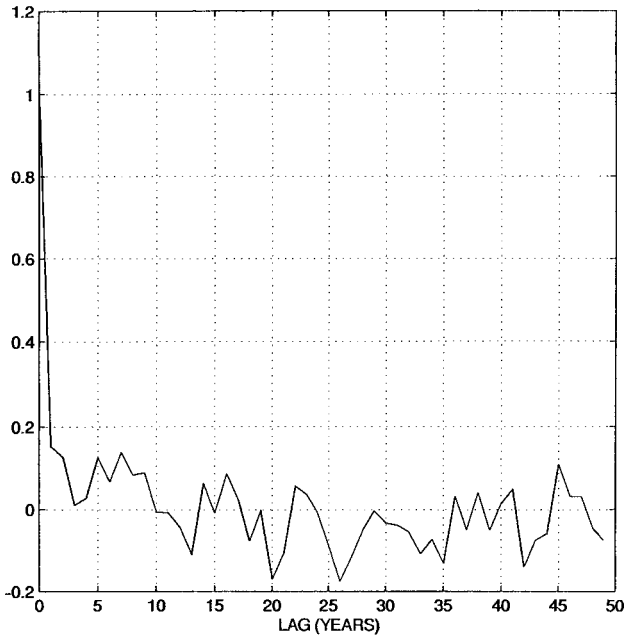

FIG. 5. Autocorrelation (normalized to 1 at zero lag) for z_t. The large value at the origin, followed by the rapid drop at lag 1 and beyond is indicative of the near-white spectral density.

larger predictive skill. Although we have not made a full attempt to determine the best value of K, a reasonable estimate is $K = 2$. Note that if z_t is actually white noise, then the standard error of r_k is about $\pm 1/(133)^{1/2} = .09$ (Jenkins and Watts 1968), a threshold (Fig. 5) that is only marginally reached (at about 67% confidence) between lags of 5 and 10 yr. Further increases in K lead to spurious skill, dependent upon covariances statistically indistinguishable from zero. With a 2-yr lag time, that is, with a knowledge of z_t, z_{t-1}, z_{t-2}, one has a predictive skill of 3.5% of the total NAO variance, shown as the prediction error in Fig. 6. Even if one made the extremely optimistic assumption that the lag-19 covariances were nonzero, the skill is little more than 10% of the total variance.

This calculation refers only to self-prediction and does not disprove the possibility that some other variable could forecast it with greater skill. It also does not prove that there is no significant nonlinear prediction possible (and the frequency function for z_t appears to be somewhat non-Gaussian). Specific wavenumber bands or other spatial structures (e.g., EOFs) in the NAO might be more predictable, but these would necessarily have only a fraction of the total NAO energy, and the present result is discouraging. Other measures of predictive skill can be developed, but it seems unlikely they will produce qualitatively different results.

5. Visual correlations

One often sees discussions of apparent visual correlations between two or more climate time series. One must be extremely careful not to be misled by oscillations that are merely the happenstance of random variability and imply no causal connection at all. The human eye developed to find patterns in nature; it sometimes sees patterns where none exist. Red noise (strongly autocorrelated) processes are particularly prone to generating oscillations that to the eye look related. Pittock's (1978) review of repeated attempts to demonstrate the existence of sunspot cycles in an endless list of physical phenomena is a sobering reminder of the consequences of seeking too hard for what one wishes to find.

Consider two time series,

$$x_t = ax_{t-1} + \theta_t,\ y_t = by_{t-1} + \eta_t. \qquad (6)$$

Here a, b are fixed numbers, such that $|a|, |b| < 1$, and θ_t, η_t are white noise processes such that $< \theta_t > = 0$, $\theta_t\theta_{t'} > = \sigma_\theta^2\delta_{tt'}$, $< \eta_t > = 0$, $< \eta_t\eta_{t'} > = \sigma_\eta^2\delta_{tt'}$, $< \theta_t\eta_{t'} > = 0$. The restrictions on a, b render x_t, y_t stationary. [Technically, x_t, y_t are autoregressive processes of order 1, denoted AR(1).] Two such time series were generated (Fig. 7) with $a = 0.999$ and $\sigma_\theta = 0.1$, $b = 0.95$,

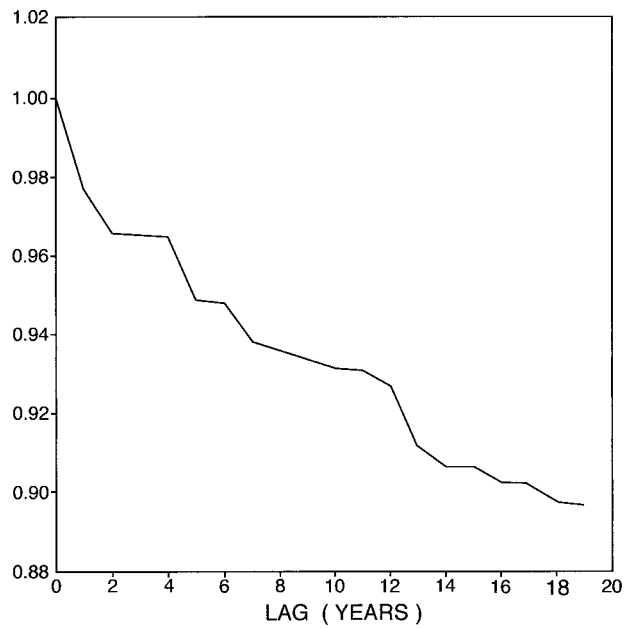

FIG. 6. Estimated prediction error variance σ_θ^2 as a function of largest lag, K for the NAO index. The probable best estimate is $K \approx 2$, suggesting that only 3%–4% of the index variance is predictable by linear means.

and $\sigma_\eta^2 = 1$. Because the two noise processes were independently generated, x_t and y_t are rigorously uncorrelated.

Both processes are red noise at high frequencies, with x_t becoming nearly white at periods longer than about 1000 time units, not unlike some geophysical processes. Here y_t has much more high-frequency energy than x_t and was thus averaged over 40 time steps before plotting to render its low frequencies visible. Three thousand values of the resulting time series are displayed in Fig. 7a. One might be tempted to conclude that the two time series are related in the time span from about 4000 to 5500.

In the example in Fig. 7a, the two time series were deliberately given different spectral structure. If they are rigorously uncorrelated, but AR(1) with the *same* structure (i.e., $a = b$, $\sigma_\eta = \sigma_\theta$), one can obtain results such as in Figs. 7b,c with visually striking apparent co-oscillations, which occur by pure chance. Jenkins and Watts (1968, 338) discuss the sample statistics of the cross covariance of two mutually uncorrelated, but individually autocorrelated, time series, and the general topic is given the label "Slutsky–Yule effect" by Kendall and Stewart (1973, 392). Many investigators further compound the difficulty by visually shifting two processes relative to each other in the time domain, and then interpret the shift as an indication of a physical time lag in the system. The opportunity for false positive results is then greatly further enhanced. Proper statistical analysis tools (coherence analysis, etc.) that the textbooks discuss would prevent one from falling into the trap of imputing relationship where none exists.

6. Comparison to the Southern Oscillation

The SO and its trends through time have recently been the subject of published debate between

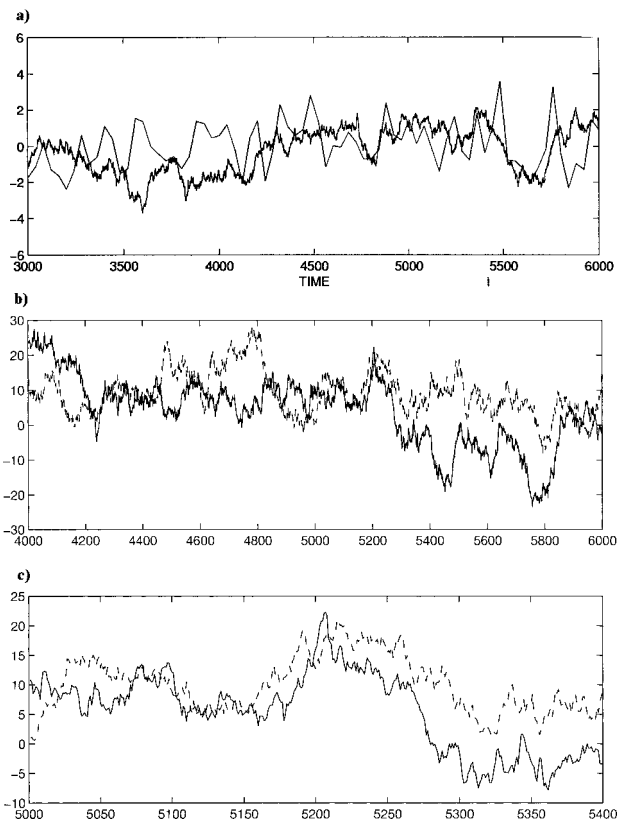

FIG. 7. (a) Two rigorously uncorrelated AR(1) processes x_t, y_t, the parameters having been described in the text. Here, y_t was filtered prior to plotting to remove much of the high-frequency energy. (b) Portion of the time history of the behavior of two rigorously uncorrelated AR(1) processes, which have identical parameters. (c) Expanded version of (b).

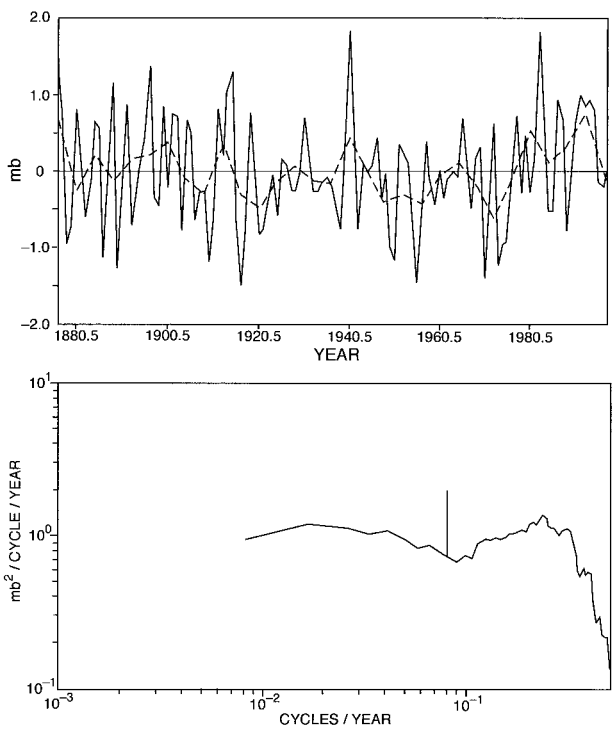

FIG. 8. (top) The Darwin pressure anomaly time series [$p_D(t)$ as an annual average and as a running 4-yr average from 1876 to 1997. The pressure minimum that occurred in early 1998 (not shown) is close to, but no smaller, than some of the extremes occurring previously in this record. (bottom) Spectral density estimate for annual average Darwin pressure. In contrast to the NAO record, here most of the energy lies in the vicinity of the weak spectral maximum centered near a 4-yr period. An approximate mean 95% confidence interval is shown.

Trenberth and Hoar (1996, 1997), Harrison and Larkin (1997), Rajagopalan et al. (1997), and others and there is no need to repeat the details of those studies. Nonetheless, a brief comparison of the NAO spectral structure with the SO is interesting and perhaps useful. Although the Southern Oscillation index (SOI) is commonly used to measure the SO, Trenberth and Hoar (1997) regard it as unreliable prior to 1935. We follow their lead and use Darwin pressure anomaly, $p_D(t)$, as a surrogate, although the simulations described below were very similar when done for the SOI [Trenberth and Hoar use $-p_D(t)$]. The top panel of Fig. 8 displays both $p_D(t)$ as an annual average and (dashed line) its 4-yr running average. The bottom panel of Fig. 8 depicts the spectral density estimate of $p_D(t)$ using the full record.

The SO spectral density is much redder than that of the NAO in the period range between about 1 and 4 yr. A broad peak centered near 4 yr is statistically significant and is an indicator of ENSO. Below the ENSO peak, the spectral density is indistinguishable from white noise. The crux of the debate over the SO alluded to above concerns the extended period of positive anomaly in the early 1990s and whether such an extended duration is indicative of a climate shift. Trenberth and Hoar (1996) generated an ARMA simulation of the SOI. Here for consistency with the discussion of the NAO, I will again use the nonparametric[2] model (see footnote 1) to generate a time series with the spectral density of the bottom panel of Fig. 8. The results for two arbitrary 120-yr intervals filtered to 4-yr averages are shown in Fig. 9. Although we will not dwell on it, it appears that sustained intervals of positive (e.g., years 3025–3085) and negative (3950–4000) values occur by chance, consistent with the inferences of Rajagopalan et al. (1997) and Harrison and Larkin (1997). The specific ARMA model of Trenberth and Hoar (1997) is probably too great an underparameterization of the time series (i.e., not sufficiently structured). They maintain, however, that the magnitude of the recent excursion of the SO is inconsistent with stationarity, and we will reexamine that conclusion in a different way in the next section.

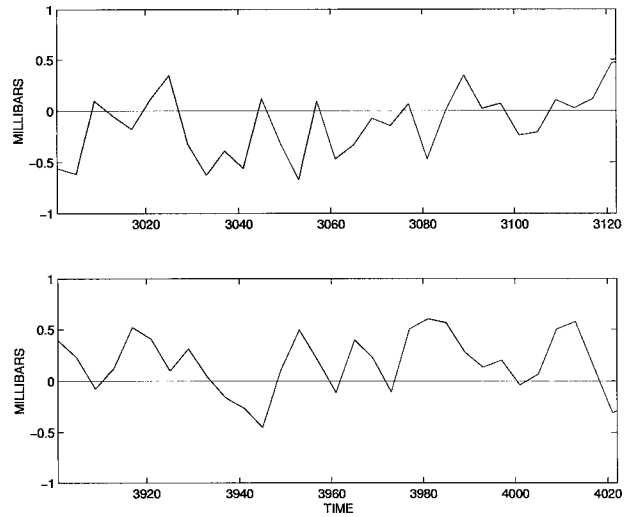

FIG. 9. Two 122-yr intervals of simulated $p_D(t)$ obtained from the observed spectral density estimate. Sustained intervals of dominantly positive and negative values and of apparent trends are clear.

7. Result from threshold crossing statistics

Threshold-crossing statistics and the statistics of extremes provide powerful tools for studying the probability that some event has occurred by chance or whether the probability appears so low that one needs to invoke a changed physical situation. The following is adapted from Vanmarcke (1981); Ponte (1986) provides a summary in the El Niño context. The wider literature is very large.

Here we will sketch a few results, focusing on the Darwin pressure series $p_D(t)$. Figure 10 redisplays the annual average $p_D(t)$ and the 4-yr average $p_{D4}(t)$ from 1876 to 1997 along with two pairs of horizontal lines denoting the one and two standard deviation limits. To qualitatively understand whether the positive values of $p_D(t)$ in the early 1990s are to be expected from a stationary, Gaussian time series, we will apply some of the machinery summarized by Vanmarcke (1981), without, however, providing a derivation.

Define the spectral moments, λ_k, of the power density spectrum of $p_D(t)$ as

$$\lambda_k = \int_0^\infty \omega^k \Phi(\omega/(2\pi))\, d\omega, \quad k = 0,1,2,\ldots. \quad (7)$$

Note the use here of radian frequency. A "spectral bandwidth" is

[2] I am using the term nonparametric in its spectral analysis sense of an ordinary Fourier component basis. This usage contrasts with parametric methods relying upon, for example, ARMA-type representations leading to maximum entropy and other spectral methods.

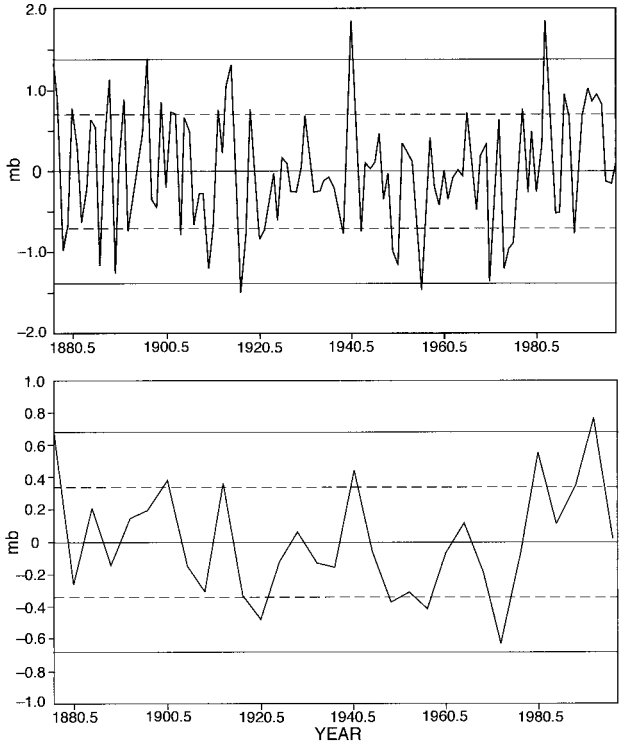

FIG. 10. (top) Annual average $p_D(t)$ replotted from Fig. 8a, with horizontal lines showing the one and two standard deviation limits, σ and 2σ. (bottom) The same as top panel except for the 4-yr values, $p_{D4}(t)$.

$$\varepsilon = \left(1 - \frac{\lambda_2^2}{\lambda_0 \lambda_4}\right)^{1/2}. \qquad (8)$$

Based upon this bandwidth and the Gaussian assumption, it is possible, among a number of properties, to calculate the mean interval between upward crossings of a threshold. The expression [Vanmarcke's Eq. (4.4.5)] depends upon the spectral moments only (not the detailed spectral shape) and the statistics of dp_D/dt as derived from the spectral moments. We find for $p_D(t)$ that the expected time interval to cross $2\sigma = 1.4$ mb is about 30 yr, implying about four crossings in 122 yr. The expected time to remain above the 2σ threshold is about 0.7 yr. The top panel of Fig. 10 shows that in the 122 yr of the record, $p_D(t)$ crosses this threshold twice and just touches it twice. If we assign the touching points as threshold crossings, there is complete consistency with the expected rate. That the expected time above the threshold is less than a year is also consistent with these results. [Omission of the last seven values of $p_D(t)$, during the 1990s, in the spectral moment calculation makes no significant difference in the numbers.]

If the same expressions are applied to $p_{D4}(t)$, the expected 2σ crossing interval is about 110 yr with an expected residence time of 2.5 yr. Figure 10 suggests that the single occurrence, toward the end of the record, is consistent with this behavior. One might regard it as peculiar that the extreme event occurred close to the end of the observation period, but there is no gainsaying that the behavior seems consistent with the theory. Grove (1998), assuming Asian monsoon behavior is a valid ENSO proxy, shows that events as extreme as the recent one have occurred in the past. It is characteristic of systems with long memory that larger deviations from the mean *are expected* as the record length grows (Feller 1957). Consequently, insofar as these tests are concerned, we have no evidence that the behavior of the SO is in any way surprising in the 1980s and 1990s, consistent with the conclusions of Harrison and Larkin (1997) and Rajagopalan et al. (1997). Again, as above, this result is not proof that a change in statistics did not occur, it is only an indication that the data do not appear to require such a conclusion; this distinction is an important one.

This discussion is not complete; there is much more that can be done with the known machinery of the statistics of extremes and of threshold crossings, including accounting (see the next section) for possible deviations from a normal probability density. An extended study of the Southern Oscillation is, however, beyond our intended scope.

8. Nonnormal statistics and nonstationarity

The assumption that the underlying statistics are nonnormally distributed introduces large new possibilities for seemingly bizarre behavior of even stationary time series, particularly if the new probability density has long tails. [Thomson (1995) has demonstrated convincing, but very subtle, nonstationarity in the periodic (nonstochastic) components of long climate records through the use of demodulation and jackknife techniques.] Consider the Gaussian time series in Fig. 11a; here x_t was produced as a simple AR(1) time series with parameter $a = 0.999$. Any nonlinear transformation of x_t,

$$y_t = g(x_t), \qquad (9)$$

will render the statistics of y_t nonnormal. As one simple example, Fig. 11b displays the result if taking

$y_t = x_t^3/1000$. The reader can readily confirm that the frequency function for x_t is transformed into a new frequency function for y_t that has much larger probabilities of extreme values. In particular, the "event" near $t = 1300$ is the result of such an occurrence. Without a study of the statistical properties of y_t, one might be tempted to conclude that some nonstationary behavior was taking place; but because of the way the time series was generated, we know it to be stationary, and we are seeing a manifestation of nonnormal statistics. Threshold-crossing statistics will be modified in the presence of such nonnormal behavior. [The reader who regards Eq. (9) and the behavior seen in Fig. 11 as extreme is reminded that many time series measurements have this visual appearance. One oceanographic example, from a current meter, is shown in Fig. 4 of Wunsch (1997), and it is widely recognized that physical processes such as tropical rainfall records have long-tailed probability distributions.]

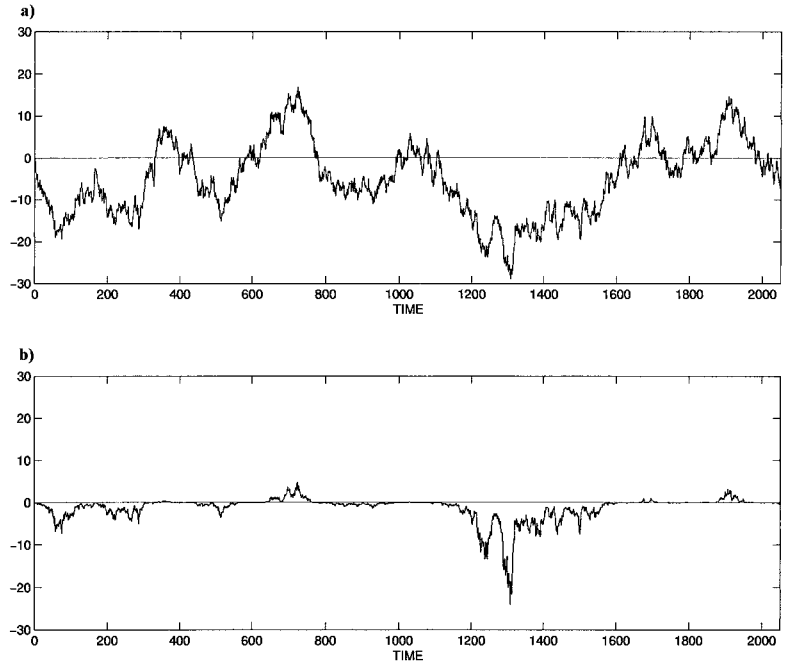

FIG. 11. (a) Normally distributed, autoregressive process, $x_t = 0.999x_{t-1} + \theta_t$. (b) Nonnormally distributed process $y_t = x_t^3/1000$. The apparently nonstationary visual behavior arises because of the non-Gaussian statistics; the time series itself remains stationary.

A further important point is that nonstationarity by itself need not imply any change in physics (emphasized by Stephenson et al. 1999). So-called autoregressive integrated moving average processes (see Box et al. 1994) generate nonstationary sequences for fixed parameters. The simplest such process is

$$x_t = x_{t-1} + \theta_t, \tag{10}$$

where θ_t is again white noise and whose variance grows with time. The rule (10) is closely connected to the fascinating "game of Peter and Paul," which is analyzed by Feller (1957).

9. Some concluding remarks

Undoubtedly the real climate record contains physically significant trends and changes in spectral shape or energy levels. Two visually but statistically insignificantly correlated climate records may well be linked in a causal manner. Caution is required, however: short records of processes that are even slightly reddish in spectral character can easily lead to unwarranted, and incorrect, inferences if simple stochastic superposition is confused with deterministic causes. As examples of the care required to draw definite conclusions about nonstationary behavior, see the studies by Thomson (1995, 1997). Sometimes there is no alternative to uncertainty except to await the arrival of more and better data.

Published inferences about a recent change in climate state appear very fragile. Nonetheless, even if no such changes have occurred, there is still much to understand about the existing climate system. For example, the weakly red nature of the NAO spectrum does produce some simple linear predictive skill; the origin of this "red" behavior and of the superimposed spectral structures needs explanation. Even if understanding does not necessarily lead directly to useful predictive skill for the NAO, it could still shed considerable light on the behavior of the coupled ocean–atmosphere system.

Similarly, the recent behavior of El Niño admits the possibility that at least some of this phenomenon is an oceanic response to purely stochastic atmospheric forcing. Ponte's (1986) discussion is along these lines, and recent papers by Blanke et al. (1997) and Eckert and Latif (1997) (or see the review by Latif

et al. 1998) lend support to the notion that one must understand possible random walk behavior before inferring that deterministic physical changes have occurred.

Nothing said here should be taken as support for an inference that climate change has not occurred nor will occur in the future. The political problem is one of risk assessment in the presence of great uncertainty. Both political and scientific progress are more likely if one is careful about what is definitively known as opposed to what are reasonable assumptions.

Acknowledgments. This research was supported in part by a grant from the National Science Foundation. I thank Jason Goodman for giving me the NAO time series and D. E. Harrison for the SO time series and discussion of these results. Comments by C. Frankignoul, D. Stephenson, and D. Schrag were very helpful. Contribution to the World Ocean Circulation Experiment.

Appendix: Prediction Error Filter

One can define a convolution inverse, b_k, to a_k in the sense

$$\sum_{k=0}^{K} a_k b_{t-k} = \delta_{t0}, \quad b_0 = 1.$$

Sequences a_k, b_k that are stable and have each other as one-sided convolution inverses, are known as "minimum phase" sequences. It is an easy matter to show that b_k, known as the prediction error filter, satisfies the equations

$$\mathbf{Rb} = \mathbf{d},$$

and $\mathbf{d}$ is found from $\mathbf{b}$.

Here

$$\mathbf{R} = \begin{Bmatrix} r_0 & r_1 & r_2 & & r_{K-1} \\ r_1 & r_0 & r_1 & & r_{K-2} \\ & & \ddots & & \\ & & & r_0 & \\ r_{K-1} & r_{K-2} & & & r_0 \end{Bmatrix}$$

is the Toeplitz matrix of the autocovariance $r_k = < z_t z_{t+k} >$, $\mathbf{d} = [\ \sigma_\theta^2\ 0\ \ 0 \cdots 0]^T$. In practice, the autocovariances are estimated from the data (Fig. 5), and the determination of K must be part of the solution itself. By the Wiener–Khinchin theorem, r_τ is the Fourier transform of $\Phi(s)$. If z_t were white noise, then $r_k = 0$, $k \neq 0$, and of necessity $\sigma_\theta^2 = \sigma^2$, that is, the prediction error would be the same as full variance of the NAO. It is only to the extent that $\Phi(s)$ is nonwhite that one has any linear predictive skill.

References

Blanke, B., J. D. Neelin, and D. Gutzler, 1997: Estimating the effect of stochastic wind stress forcing on ENSO irregularity. *J. Climate,* **10,** 1473–1486.

Box, G. E. P., G. M. Jenkins, and G. C. Reinsel, 1994: *Time Series Analysis. Forecasting and Control.* 3d ed. Prentice-Hall, 598 pp.

Claerbout, J. F., 1976: *Fundamentals of Geophysical Data Processing. With Applications to Petroleum Prospecting.* McGraw-Hill, 274 pp.

Eckert, C., and M. Latif, 1997: Predictability of a stochastically forced hybrid coupled model of El Niño. *J. Climate,* **10,** 1488–1504.

Feller, W., 1957: *An Introduction to Probability Theory and Its Applications.* 2d ed. Wiley, 461 pp.

Frankignoul, C., and K. Hasselmann, 1977: Stochastic climate models. Part II. Application to seasurface temperature, temperature anomalies and thermocline variability. *Tellus,* **29,** 289–305.

Goodman, J., cited 1997: Spectral analysis of NAO time series. [Available online at http://-www.mit.edu/people/goodmanj/NAOI/.]

Grove, R. H., 1998: Global impact of the 1789–93 El Niño. *Nature,* **393,** 318–319.

Harrison, D. E., and N. K. Larkin, 1997: Darwin sea level pressure, 1876–1996: Evidence for climate change? *Geophys. Res. Lett.,* **24,** 1775–1782.

Hasselmann, K., 1976: Stochastic climate models. Part 1. Theory. *Tellus,* **28,** 473–485.

Hurrell, J. W., 1995: Decadal trends in the North Atlantic oscillation regional temperatures and precipitation. *Science,* **269,** 676–679.

——, and H. van Loon, 1997: Decadal variations in climate associated with the North Atlantic Oscillation. *Climate Change.,* **36,** 301–326.

Jenkins, G. M., and D. G. Watts, 1968: *Spectral Analysis and Its Applications.* Holden-Day, 525 pp.

Kendall, M. G., and A. Stuart, 1973: *The Advanced Theory of Statistics.* 3d ed. Vol. III. Griffin, 585 pp.

Latif, M., D. Anderson, T. Barnett, M. Cane, R. Kleeman, A. Leetmaa, J. O'Brien, A. Rosati, and E. Schneider, 1998: A review of the predictability and prediction of ENSO. *J. Geophys. Res.,* **103,** 14 375–14 394.

Levinson, N., 1947: The Wiener RMS (root mean square) error criterion in filter design and prediction. *J. Math. Phys.,* **25,** 261–278.

Percival, D. B., and A. T. Walden, 1993: *Spectral Analysis for Physical Applications. Multitaper and Conventional Univariate Techniques.* Cambridge University Press, 583 pp.

Pittock, A. B., 1978: A critical look at long-term sun-weather relations. *Rev. Geophys. Space Phys.,* **16,** 400–420.

Ponte, R. M., 1986: The statistics of extremes, with application to El Niño. *Rev. Geophys.,* **24,** 285–297.

Rajagopalan, B., U. Lall, and M. A. Cane, 1997: Anomalous ENSO occurrences: An alternative view. *J. Climate,* **10,** 2351–2357.

Rice, S. O., 1945: Mathematical analysis of random noise. *Bell Sys. Tech. J.,* **25,** 46–156.

Stephenson, D. B., V. Pavan, and R. Bojariu, 1999: Is the North Atlantic Oscillation a random walk? *Int. J. Climatol.,* in press.

Thomson, D. J., 1995: The seasons, global temperature, and precession. *Science,* **268,** 59–68.

——, 1997: Dependence of global temperatures on atmospheric CO_2 and solar irradiance. *Proc. Natl. Acad. Sci. USA,* **94,** 8370–8377.

Trenberth, K. E., and T. J. Hoar, 1996: The 1990–1995 El Niño Southern Oscillation event: Longest on record. *Geophys. Res. Lett.,* **23,** 57–60.

——, and ——, 1997: El Niño and climate change. *Geophys. Res. Lett.,* **24,** 3057–3060.

Vanmarcke, E., 1983: *Random Fields: Analysis and Synthesis.* The MIT Press, 382 pp.

Wunsch, C., 1992: Decade-to-century changes in the ocean circulation. *Oceanography,* **5,** 99–106.

——, 1997: The vertical partition of oceanic horizontal kinetic energy. *J. Phys. Oceanogr.,* **27,** 1770–1794.